International Journal of Current Science Research and Review
ISSN: 2581-8341
Volume 07 Issue 10 October 2024
DOI: 10.47191/ijcsrr/V7-i10-17, Impact Factor: 7.943
IJCSRR @ 2024
www.ijcsrr.org

A Simplified Dynamic Model of DFIG-based Wind Generation for Frequency Support Control Studies

Anjie Jiang
North Carolina State University, Raleigh, NC 27695

ABSTRACT: In recent years, wind generation has been fast growing and become one of the major generation resources in power systems. Since the wind generation does not inherently equip with frequency support functions, the power system frequency response degrades as the wind penetration increases. Therefore, frequency support control of wind generation has gained increasing focus. However, the dynamic models of wind generation systems, which are required by the control design and analysis, are commonly very complicated and difficult to obtain, especially for the doubly-fed induction generator based wind turbine (DFIG-WT). In this paper, the authors propose a simplified dynamic model for the DFIG-WT. The proposed analytical model is derived from the detailed model by selectively neglecting very fast dynamics while keeping the critical ones. It is suitable for frequency control studies. The model accuracy is first validated against the detailed DFIG-WT model in Simulink. Then, the wind frequency control function is studied based on the proposed model.

KEYWORDS: Dynamic Model, DFIG, Studies

INTRODUCTION

As one of the most commonly utilized renewable energy resources, wind generation has now become an essential part of modern power system. It usually provides clean electricity to the grid through induction generator, as well as power electronic devices. According to IEA's statistics, the worldwide wind generation capacity has reached 736 GW by 2021, amounting 24.8% of the total renewable generation capacity 0. However, similar to PV, wind generation typically does not have any frequency support capability such as inertial or droop response from synchronous generators 2. As a result, the frequency response degrades in a high renewable penetration power system 3. Several approaches have been proposed by the researchers to enable wind generation to participate in frequency support control.

Instead of using conventional maximum power point tracking (MPPT) control, setting the power-speed characteristics below the MPPT curve is commonly used to reserve certain power for supporting the frequency 4. In this approach, the wind output power can be adjusted in response to frequency disturbances. Authors in 5 suggests a new suboptimal power point tracking characteristics for wind generation to follow, where the deloaded power is set differently at low and high wind speeds. The inertia and droop emulation control is then implemented. Another approach relies on utilizing the stored kinetic energy in wind turbine's rotor. This is similar to the inherent inertial response of synchronous generators. In 6, the authors modify the MPPT curve according to the frequency change so that the wind turbine operates from conventional MPPT points to the new ones. By doing so, the new operating point corresponds to similar mechanical power input, which equals to the steady-state electrical power output, while the rotor speed goes up or down to absorb or release power during the dynamics. The above are heuristic methods which are not model-derived. The main drawback is the incapability to perform analytical studies, and thus guarantee the dynamic performance.

To overcome the above limitation, an analytical wind turbine model suitable for frequency control study is needed. However, many of the existing models are too complicated with high orders, especially for doubly-fed induction generator based wind turbine (DFIG-WT), also referred to as type-3 wind turbine 7, which has gained much of interest for its advantages on wider operation speed range and advanced control functions. Different than other types of wind turbines, the DFIG-WT has two ways of power flow from the turbine to grid: one is through the induction generator that is directly grid-connected; the other one is through back-to-back converters.

Detailed modelling of DFIG-WT involves many dynamic states from the induction generator, rotor-side converter (RSC), DC-link, and grid-side converter (GSC). 8 gives a detailed model for the induction generator used in DFIG-WT but does not consider the

International Journal of Current Science Research and Review
ISSN: 2581-8341
Volume 07 Issue 10 October 2024
DOI: 10.47191/ijcsrr/V7-i10-17, Impact Factor: 7.943
IJCSRR @ 2024
www.ijcsrr.org

converters. Authors in 9 uses equivalent circuit to represent the induction generator and derives the small-signal model of DFIG-WT including the converters. However, the model is still excessively complicated, and its validation is not justified in the paper. A simplified model is proposed in 10 for DFIG-WT with virtual synchronous control. However, this model is over-simplified with no converter dynamics considered.

To enhance wind turbine control and modeling, recent innovations in AI, machine learning, and simulation techniques have shown promise. For instance, self-adaptive robust motion planning techniques have been applied to robotic systems, demonstrating improvements in dynamic control that can also be adapted to wind turbine systems [11]. Similarly, enhancing the authenticity and accuracy of data inputs for wind turbine control models is critical, especially in the context of complex system dynamics [12]. Additionally, ensemble methodologies combining LightGBM, XGBoost, and other local ensembles have been suggested for predictive maintenance, helping to forecast failures and reduce downtime in wind systems [13]. Image-based techniques like MRI scan segmentation algorithms can be adapted to monitor turbine component health and identify anomalies before they lead to major failures [14]. The paper "DRAL: Deep Reinforcement Adaptive Learning for Multi-UAVs Navigation in Unknown Indoor Environment" explores how a deep learning algorithm enables drones to autonomously navigate using a single camera, suggesting its potential to enhance adaptive control systems in wind turbines for improved performance under dynamic conditions[15].

Generally, different studies may have different preferences on the model to apply. Therefore, for analyzing wind generation's frequency support control, a suitable dynamic model can ignore the dynamics which are much faster than the normal system frequency dynamics and keep those dominant ones at the corresponding timescale. Following this idea, we propose a simplified dynamic model for DFIG-WT. This model is suitable for frequency support control design as its dynamic order is reduced, and it has the appropriate control input variable with physical meaning.

1. DFIG-WT

Recently, out of many configurations of wind turbine, the DFIG-WT has become very popular as one of the variable speed wind generations 14. The diagram for DFIG-WT is as illustrated in Fig. 1. Compared to other configurations with converters involved such as the Type-4 with full converter unit, a clear advantage of DFIG-WT is that the converters only need to handle a friction (20% – 30%) of the rated power 17. In this way, the losses, as well as the cost, of converters can be greatly reduced 18.

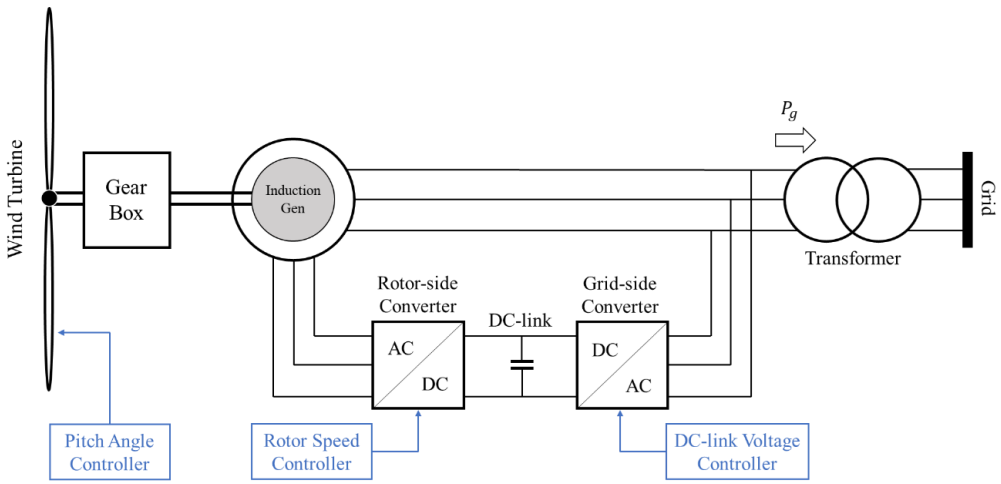

Figure 1. Diagram of a grid-connected DFIG-WT

For the control of a DFIG-WT, three controllers can be categorized, namely: pitch angle controller, rotor speed controller, and DC-link voltage controller. With the help of these controllers, the wind turbine can stably operate at different zones. In Fig. 2, the solid lines represent the mechanical power input to the turbine at different rotor speeds, while the dashed lines represent the operating zones. The wind turbine does not generate power until rotor speed reaches 0.7 p.u.. Then, with very little increase of ω_r, the electrical power, which is equal to mechanical power input, climbs up from A to B. Segment B-C is commonly referred to as the optimal

International Journal of Current Science Research and Review
ISSN: 2581-8341
Volume 07 Issue 10 October 2024
DOI: 10.47191/ijcsrr/V7-i10-17, Impact Factor: 7.943
IJCSRR @ 2024
www.ijcsrr.org

zone, where it connects the maximum mechanical power point at different wind speeds. The optimal zone is usually tracked for maximum extraction of wind power, and it is realized by the RSC controller. The controller takes the feedback of ω_r and returns power reference to regulate the rotor's electrical torque according to segment B-C. During this stage, the pitch angle is kept constant at zero. When rotor speed reaches 1.2 p.u., the pitch angle controller controls the angle to regulate the mechanical power input at rated power. In the meantime, the DC-link voltage controller regulates the DC-link capacitor's voltage, so that the power changes on the rotor can be reflected to the grid through GSC.

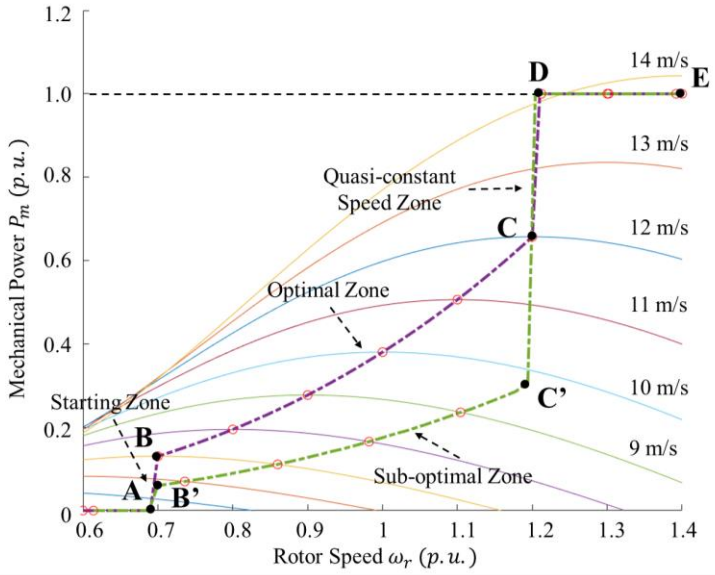

Figure 2. Power-speed characteristics and operating zones of wind turbine

Other than normal conditions, a DFIG-WT with frequency support functions should operate at a deloaded condition, which is segment B'-C'. Demonstrated by Fig. 2, the so-called sub-optimal zone corresponds to lower power than the optimal zone. Here we adopt the method in 5 for the deloading. When operating in B'-C', the wind turbine can adjust its output power in response to frequency changes.

2. Simplified Dynamic Model

To derive a simplified dynamic model for DFIG-WT in Fig. 1, we first need to select the critical dynamics. Since the model is used primarily for frequency support studies, where the wind turbine operates at segment B'-C' in Fig. 2, we can ignore the pitch angle controller which is inactive in this zone. In addition, we ignore the DC-link voltage controller as it's dynamics are fast and do not have significant impact on the output power. Specifically, we keep the dynamics of wind turbine, rotor, RSC, and RSC controller in the simplified model, as illustrated by Fig. 3.

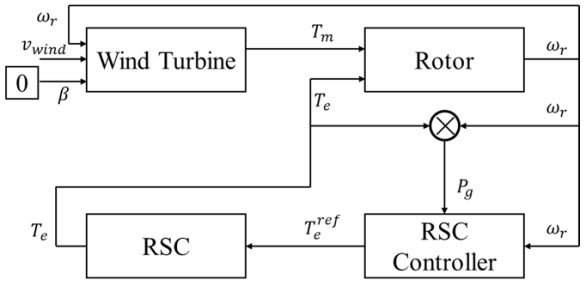

Figure 3. Control diagram for the simplified model

International Journal of Current Science Research and Review
ISSN: 2581-8341
Volume 07 Issue 10 October 2024
DOI: 10.47191/ijcsrr/V7-i10-17, Impact Factor: 7.943
IJCSRR @ 2024
www.ijcsrr.org

2.1. Wind Turbine

The wind turbine block models the relationship among mechanical power (or torque) input, wind speed, rotor speed, and pitch angle. Since the model is for sub-optimal zone, pitch angle is fixed at 0. The relationship essentially represents the collection of solid lines for various wind speeds as shown in Fig. 2. A discussion on the analytical representation of the relationship can be found in 19, but it is highly nonlinear and complicated. A more practically efficient way is to use look-up-table (LUT). Here we represent this LUT by a function so that the wind turbine can be modelled as:

$$T_m = f(\omega_r, v_{wind}) \tag{1}$$

2.2. Rotor

The rotor dynamics mainly involves with the speed changes in response to electrical and mechanical torque mismatches:

$$\dot{\omega_r} = \frac{1}{J_{eq}}(T_m - T_e) \tag{2}$$

where J_{eq} is the moment of inertia of rotor, T_e is the electrical torque.

2.3. RSC

The role of RSC is to generate relevant PWM signals such that the T_e on the rotor can follow its reference T_e^{ref}. Since the converter dynamics are very fast, we can simplify them into one delay function as:

$$T_e = \left(\frac{1}{1+\tau s}\right) T_e^{ref} \tag{3}$$

where τ is the delay time constant which should be sufficiently small, and s is the Laplace operator.

2.4. RSC Controller

For RSC controller, it receives P_g and ω_r as the feedback and generate corresponding reference signal for T_e. The controller diagram is as Fig. 4. The ω_r is first mapped to P_g^{ref} according to the sub-optimal characteristics. Then, a supervisory control input ΔP_g is added to enable frequency support control design. The output power is then compared with the composite reference ($P_g^{ref} + \Delta P_g^{ref}$) to generate the error signal. A PI controller is applied to eliminate this error and its output is T_e^{ref}. The RSC controller is modelled as:

$$T_e^{ref} = \left(K_p + \frac{K_i}{s}\right)(P_g^{ref} + \Delta P_g^{ref} - P_g) \tag{4}$$

$$P_g^{ref} = g(\omega_r) \tag{5}$$

where function g is another LUT representing the sub-optimal operating zone. K_p and K_i are the PI controller parameters.

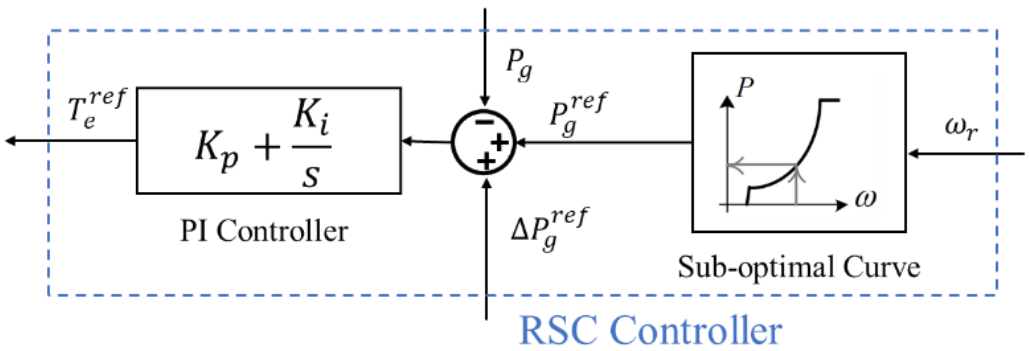

Figure 4. Control diagram for RSC controller

International Journal of Current Science Research and Review
ISSN: 2581-8341
Volume 07 Issue 10 October 2024
DOI: 10.47191/ijcsrr/V7-i10-17, Impact Factor: 7.943
IJCSRR @ 2024
www.ijcsrr.org

2.5. Complete Model

Combining equations (1)-(5) and writing in state-space form, we can have the complete simplified dynamic model for a DFIG-WT.

$$\begin{cases} \dot{\omega}_r = \dfrac{1}{J_{eq}}\left(f(\omega_r, v_{wind}) - T_e\right) \\ \dot{T}_e = \dfrac{1}{\tau}\left(-T_e - K_p T_e \omega_r + K_p\left(g(\omega_r) + \Delta P_g^{ref}\right) + K_i x\right) \\ \dot{x} = -T_e \omega_r + g(\omega_r) + \Delta P_g^{ref} \end{cases} \tag{6}$$

This simplified model has only 3 states: rotor speed ω_r, electrical torque T_e, and controller internal state x which is introduced to avoid 2nd-order terms in the model. The model has two inputs: wind speed v_{wind} and power adjustment ΔP_g^{ref}, while the later one is control input. Supervisory frequency control functions can be designed through ΔP_g^{ref}.

3. FREQUENCY SUPPORT CONTROL STUDIES

For a conventional synchronous generator, its frequency support control comprises inertial and droop responses, which can be described by:

$$\Delta P_{inertia} = -2H\omega_0 \frac{d\Delta\omega}{dt} = -K_H \frac{d\Delta\omega}{dt} \tag{7}$$

$$\Delta P_{droop} = -\frac{1}{R}\Delta\omega = -K_D \Delta\omega \tag{8}$$

where H is the system equivalent inertia constant, ω_0 is the norminal system frequency, $\Delta\omega$ is the frequency deviation, and R is the droop constant.

Similarly, as we want the DFIG-WT to change its power in response of frequency deviation, we can emulate the synchronous generator by setting the control input ΔP_g as per equation (7) and (8). In this way, the power change control signal related to frequency is sent to DFIG-WT. The control diagram is as Fig. 5. The coefficients K_H and K_D are the emulated inertia and droop constants of DFIG-WT, respectively.

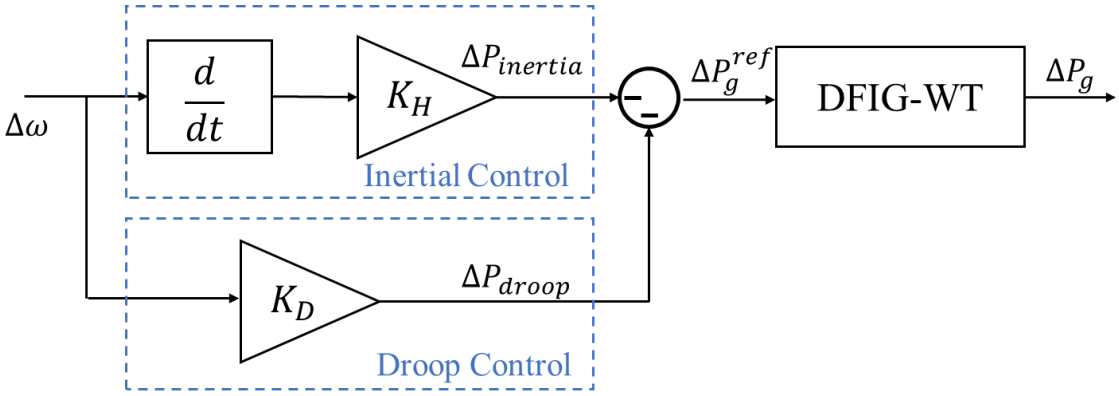

Figure 5. Control diagram for frequency support control of DFIG-WT

With the help of proposed simplified DFIG-WT model, we can further construct a complete system model to study the effectiveness of the controller. In this complete model, as shown in Fig. 6, we use the classical load frequency control model (LFC) to represent the frequency dynamics of the power system. The LFC model incorporates with wind generation by fetching increment power of wind into the power balance to reflect its impact on frequency.

International Journal of Current Science Research and Review
ISSN: 2581-8341
Volume 07 Issue 10 October 2024
DOI: 10.47191/ijcsrr/V7-i10-17, Impact Factor: 7.943
IJCSRR @ 2024
www.ijcsrr.org

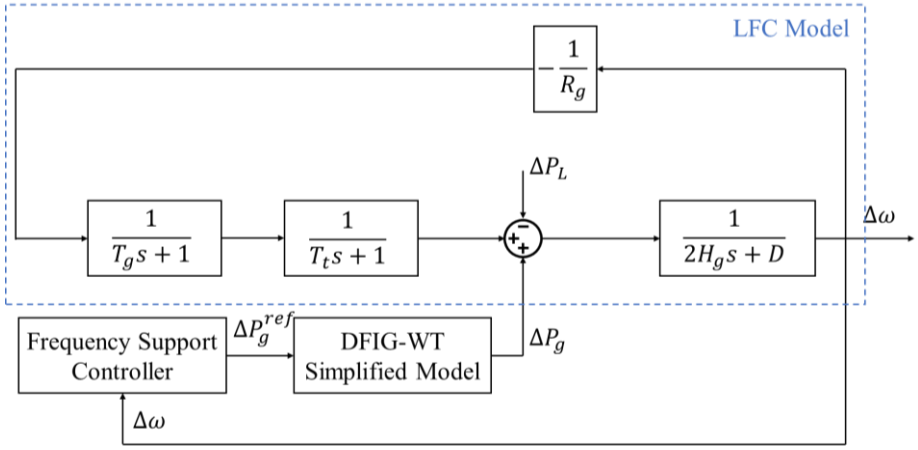

Figure 6. Complete system model used for frequency support control studies

4. TEST RESULTS

4.1. Model Validation

To validate our simplified model, we compare its dynamic performance with the detailed DFIG-WT model in MATLAB Simulink. In the simulation, we choose two disturbance events: 1) a step change in wind speed; 2) a step change in ΔP_g. For each event, we compare the rotor speed and output power from the two models. In Fig. 7, we plot the results from the first event. The wind speed drops from 11 m/s to 8 m/s at 20 s. Due to the sub-optimal curve in Fig. 2, both rotor speed and output power drop as the mechanical input power curve at 8 m/s is lower than that at 11 m/s. It is clear to see that the simplified model provides very close approximation to the detailed model. The error is barely visible.

For the second event, we give a step increase of 0.25 p.u. for ΔP_g^{ref}. As the wind turbine is initially operating at sub-optimal mode, it is feasible to increase its output power. However, since the ΔP_g^{ref} is added upon the sub-optimal curve, the P_g^{ref} as a function of ω_r also changes as the rotor speed changes. Therefore, the actual increase of output power does not equal to ΔP_g^{ref}. The spike right after the event is mainly due to the sudden drop of rotor speed, as it is releasing the kinetic energy. Similarly, for this type of event, our simplified model also demonstrates very good performance as indicated in Fig. 8.

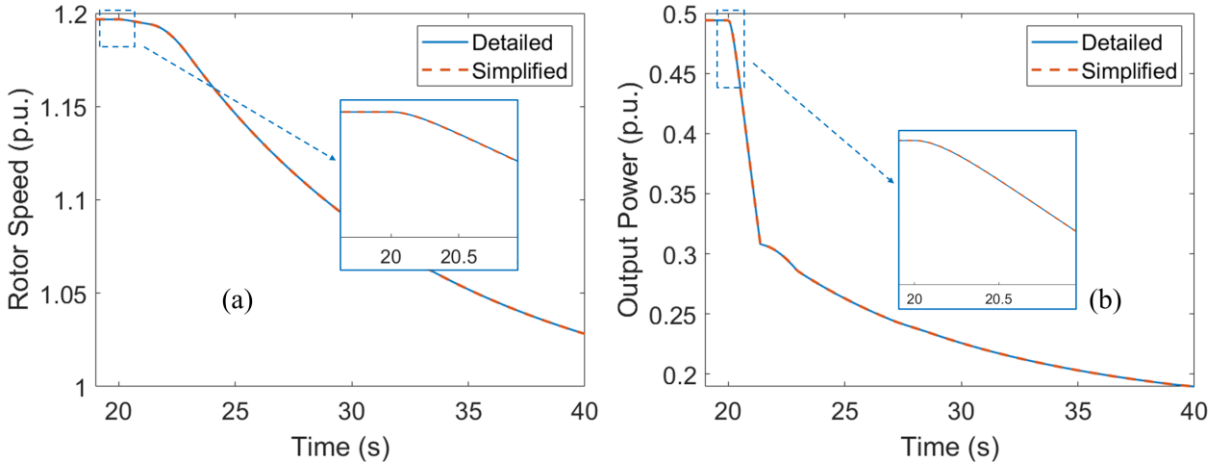

Figure 7. Comparison between detailed and simplified models under the change of wind speed: (a) rotor speed; (b) output power

International Journal of Current Science Research and Review
ISSN: 2581-8341
Volume 07 Issue 10 October 2024
DOI: 10.47191/ijcsrr/V7-i10-17, Impact Factor: 7.943
IJCSRR @ 2024
www.ijcsrr.org

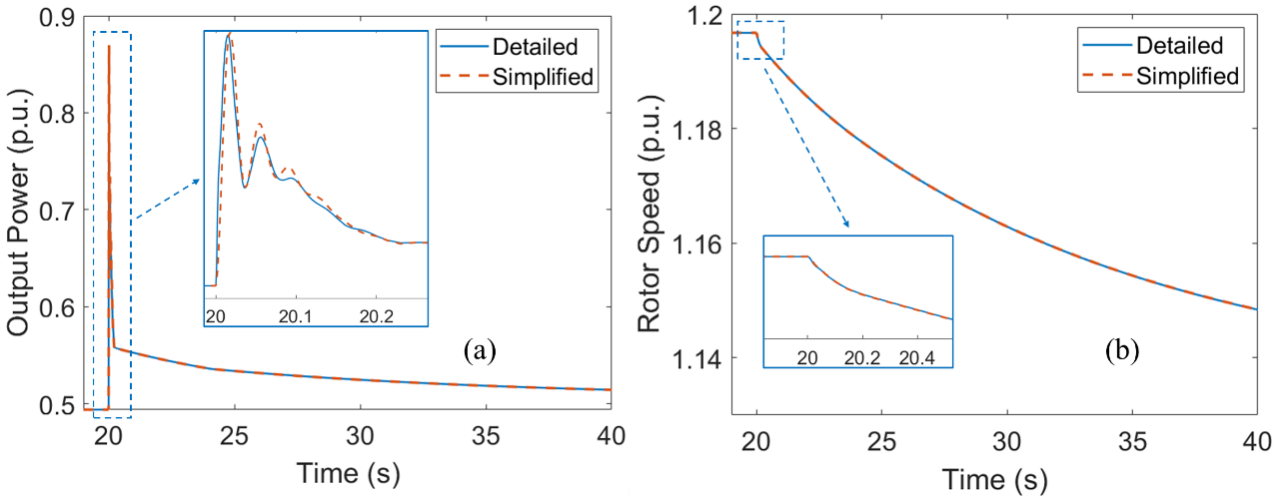

Figure 8. Comparison between detailed and simplified models under the change of ΔP_g^{ref}: (a) rotor speed; (b) output power

4.2. Frequency Support Control Studies

To test the frequency support controller using our proposed simplified model, we build the test system according to the complete system model in Fig. 6. The system is assumed to be a small-scale regional power system with base MVA being 100 MVA which is about 10 times of the wind generation capacity. In this way, the effectiveness of frequency support is easier to observe. Then, we perturb the system with an increase of 0.1 p.u. of load. Under this event, we test the system in three cases: (1) without frequency support control; (2) frequency support with lower emulated inertia and droop; (3) frequency support with higher emulated inertia and droop. The test results are in Fig. 9 and Fig. 10.\

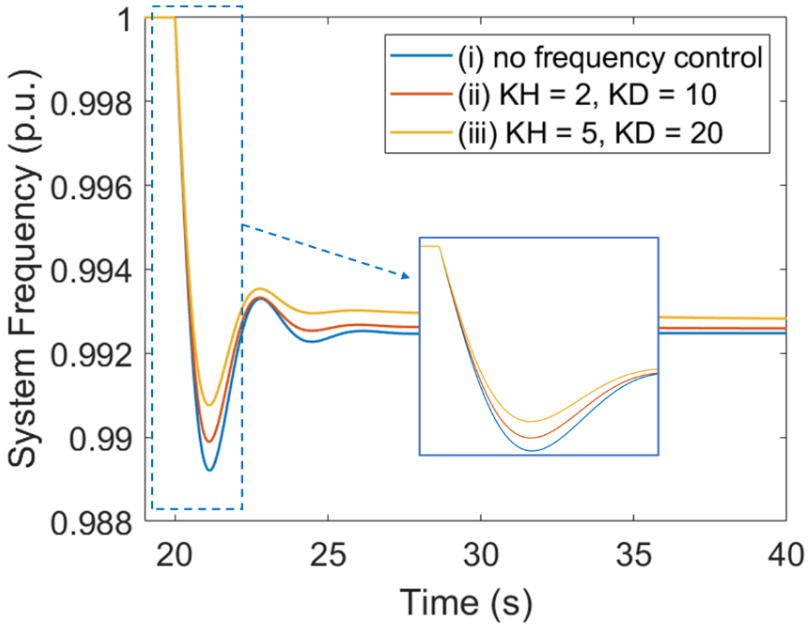

Figure 9. System frequency dynamics under the load change.

International Journal of Current Science Research and Review
ISSN: 2581-8341
Volume 07 Issue 10 October 2024
DOI: 10.47191/ijcsrr/V7-i10-17, Impact Factor: 7.943
IJCSRR @ 2024
www.ijcsrr.org

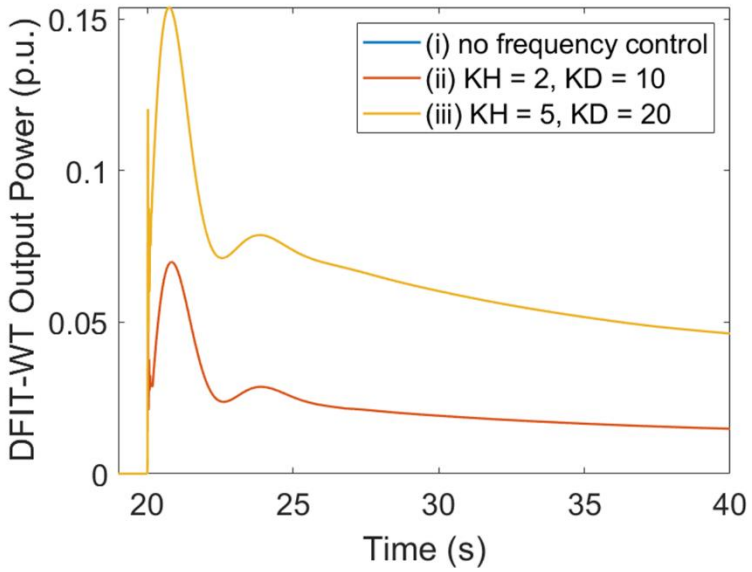

Figure 10. Wind output power change during the load change event.

Fig. 9 plots the system frequencies for the three cases under the same event. It is clear that the frequency responses of case (ii) and (iii) have been improved from that of case (i), in terms of the rate of change of frequency, nadir, and settling frequency. Furthermore, case (iii) is better than (ii) as expected, since the emulated inertia and droop coefficients are larger. In support of results in Fig. 9, Fig. 10 demonstrates the corresponding power change of wind generation. In case (i), since no control is implemented, the wind turbine does not respond to frequency event, therefore, its output power remains constant. In case (ii) and (iii), the frequency support controller changes the power reference of DFIG-WT according to $\Delta\omega$. There are power spikes right after the event, due to the sudden drop of frequency. Again, as we expected, case (iii) with the higher emulated inertia and droop leads to higher increase of output power to support the better frequency response.

5. CONCLUSIONS

In this paper, we propose a simplified dynamic model of DFIG-WT for frequency support control studies. In this model, we neglect some dynamics which are too fast to place observable impact on the turbine power and rotor speed dynamics. While the model order is reduced to only 3, this model validated for its accuracy on representing the dynamics of a DFIG-WT under the change of power reference and wind speed. Furthermore, we tested the effectiveness of this simplified model in the application of study on frequency support control, where the DFIG-WT is controlled to emulate inertial and droop responses. The simplified model with designed controller demonstrates expected and satisfactory improvement on the system frequency response.

REFERENCES

1. IEA (2021), Renewables 2021, IEA, Paris https://www.iea.org/reports/renewables-2021
2. Q. Li and M. E. Baran, "A Novel Frequency Support Control Method for PV Plants Using Tracking LQR," in IEEE Transactions on Sustainable Energy, vol. 11, no. 4, pp. 2263-2273, Oct. 2020.
3. Q. Li and S. Abhyankar, "Evaluation of High Solar Penetration Impact on Bulk System Stability through a Transmission-Distribution Dynamics Co-simulation," 2019 IEEE Power & Energy Society General Meeting (PESGM), 2019, pp. 1-5.
4. X. Zhao, Y. Xue and X. -P. Zhang, "Fast Frequency Support From Wind Turbine Systems by Arresting Frequency Nadir Close to Settling Frequency," in IEEE Open Access Journal of Power and Energy, vol. 7, pp. 191-202, 2020, doi: 10.1109/OAJPE.2020.2996949.

International Journal of Current Science Research and Review
ISSN: 2581-8341
Volume 07 Issue 10 October 2024
DOI: 10.47191/ijcsrr/V7-i10-17, Impact Factor: 7.943
IJCSRR @ 2024
www.ijcsrr.org

5. Y. Tan, L. Meegahapola and K. M. Muttaqi, "A Suboptimal Power-Point-Tracking-Based Primary Frequency Response Strategy for DFIGs in Hybrid Remote Area Power Supply Systems," in IEEE Transactions on Energy Conversion, vol. 31, no. 1, pp. 93-105, March 2016, doi: 10.1109/TEC.2015.2476827.
6. D. Ochoa and S. Martinez, "Fast-Frequency Response Provided by DFIG-Wind Turbines and its Impact on the Grid," in IEEE Transactions on Power Systems, vol. 32, no. 5, pp. 4002-4011, Sept. 2017, doi: 10.1109/TPWRS.2016.2636374.
7. Pourbeik, Pouyan. "Proposed changes to the WECC WT3 generic model for type 3 wind turbine generators." Prepared under Subcontract No. NFT-1-11342-01 with NREL, Issued to WECC REMTF and IEC TC88 WG27 12.16 (2013): 11.
8. Pulgar-Painemal, Hector A., and Peter W. Sauer. "Doubly-fed induction machine in wind power generation." Electrical Manufacturing and Coil Winding Exposition. Vol. 4. 2009.
9. Liu, Y., et al. "Frequency control of DFIG-based wind power penetrated power systems using switching angle controller and AGC." IEEE Transactions on Power Systems 32.2 (2016): 1553-1567.
10. Wang, Shuo, et al. "On inertial dynamics of virtual-synchronous-controlled DFIG-based wind turbines." IEEE Transactions on Energy Conversion 30.4 (2015): 1691-1702.
11. Y. Zhang, K. Mo, F. Shen, X. Xu, X. Zhang, J. Yu, and C. Yu, “Self-adaptive robust motion planning for high dof robot manipulator using deep mpc,” arXiv preprint arXiv:2407.12887, 2024.
12. Y. Zhang, Q. Leng, M. Zhu, R. Ding, Y. Wu, J. Song, and Y. Gong, “Enhancing text authenticity: A novel hybrid approach for ai-generated text detection,” arXiv preprint arXiv:2406.06558, 2024.
13. M. Zhu, Y. Zhang, Y. Gong, K. Xing, X. Yan, and J. Song, “Ensemble methodology: Innovations in credit default prediction using lightgbm, xgboost, and localensemble,” arXiv preprint arXiv:2402.17979, 2024.
14. Y. Zhang, Y. Gong, D. Cui, X. Li, and X. Shen, “Deepgi: An automated approach for gastrointestinal tract segmentation in mri scans,” arXiv preprint arXiv:2401.15354, 2024.
15. K. Mo, L. Chu, X. Zhang, X. Su, Y. Qian, Y. Ou, and W. Pretorius, "DRAL: Deep Reinforcement Adaptive Learning for Multi-UAVs Navigation in Unknown Indoor Environment," *arXiv preprint arXiv:2409.03930*, 2024.
16. Petersson, Andreas. Analysis, modeling and control of doubly-fed induction generators for wind turbines. Chalmers Tekniska Hogskola (Sweden), 2005.
17. L. H. Hansen, L. Helle, F. Blaabjerg, E. Ritchie, S. Munk-Nielsen, H. Bindner, P. Sørensen, and B. Bak-Jensen, “Conceptual survey of generators and power electronics for wind turbines,” Risø National Laboratory, Roskilde, Denmark, Tech. Rep. Risø-R-1205(EN), ISBN 87-550-2743-8, Dec. 2001.
18. L. Xu and C. Wei, “Torque and reactive power control of a doubly fed induction machine by position sensorless scheme,” IEEE Trans. Ind. Applicat., vol. 31, no. 3, pp. 636–642, May/June 1995.
19. Wang, Siqi, and Kevin Tomsovic. "A novel active power control framework for wind turbine generators to improve frequency response." IEEE Transactions on Power Systems 33.6 (2018): 6579-6589.

Cite this Article: Anjie Jiang (2024). A Simplified Dynamic Model of DFIG-based Wind Generation for Frequency Support Control Studies. International Journal of Current Science Research and Review, 7(10), 7617-7625, DOI: https://doi.org/10.47191/ijcsrr/V7-i10-17